

1 **Isotopic differences of soil-plant-atmosphere continuum**
2 **composition and control factors of different vegetation zones**
3 **in north slope of Qilian Mountains**

4 Yuwei Liu^{a,b}, Guofeng Zhu^{a,b,*}, Zhuanxia Zhang^{a,b}, Zhigang Sun^{a,b}, Leilei Yong^{a,b},
5 Liyuan Sang^{a,b}, Lei Wang^{a,b}, Kailiang Zhao^{a,b}

6 a School of Geography and Environment Science, Northwest Normal University, Lanzhou 730070,
7 Gansu, China

8 b Shiyang River Ecological Environment Observation Station, Northwest Normal University, Lanzhou
9 730070, Gansu, China

10 *Correspondence to:* Guofeng Zhu (gfzhu@lzb. ac.cn)

11 **Abstract:** Understanding the differences and control factors of stable water isotopes in the
12 soil-plant-atmosphere continuum (SPAC) of different vegetation zones is of great significance to reveal
13 hydrological processes and regional water cycle mechanisms. From April 2018 to October 2019, we
14 collected 1281 samples to investigated the stable water isotopes changes in the SPAC of three different
15 vegetation zones (alpine meadows, forests, and arid foothills) in the Shiyang River Basin. The results
16 show that: (1) Precipitation plays a major control role in the SPAC. From alpine meadows to arid
17 foothills, the temperature effect of precipitation isotopes increases as altitude decreases . (2) From the
18 alpine meadow to the arid foothills, soil water isotopes are gradually enriched (3) Alpine meadow
19 plants are mainly supplied by precipitation in the rainy season, and forest plants mainly utilize soil
20 water in the dry season and precipitation in the rainy season. The soil water in the arid foothills is
21 primarily recharged by groundwater, and the evaporation of plant isotopes is strong. (4) Temperature
22 and altitude are potential factors that control the isotopic composition of SPAC. This research will help
23 understand the SPAC system's water cycle at different altitudes and climates in high mountains.

24 **Keywords:** Shiyang River Basin; Stable water isotope; Precipitation; Soil water; Plant water

25 **1 Introduction**

26 The relative abundance changes of hydrogen and oxygen isotopes in water can indicate the water
27 cycle and the water use mechanism in plants, so isotope technology has become an increasingly

28 important method to study the water cycle (Gao et al., 2009; Song et al., 2002; Coplen, 2013; Shou et
29 al., 2013). The stable water isotopic composition is considered to be the "fingerprint" of water, which
30 records a large amount of environmental information that comprehensively reflects the geochemical
31 process of each system, and links the composition characteristics of each link (Darling et al., 2003;
32 Raco et al., 2013; Nlend et al., 2020). As an effective tool, stable isotope technology is widely applied
33 in studying the relationship between environmental factors and the water cycle (Araguás-Araguás et al.,
34 1998; Christopher et al., 2009), water transportation, and distribution mechanisms (Gao et al., 2011),
35 and ways of tracing water use by plants (Detjen et al., 2015). The understanding of the relationship
36 between the influence of plant characteristics, water use efficiency and water sources (Ehleringer, 1991;
37 Sun et al., 2005; Li et al., 2019) provides a new observation method for revealing the mechanism of
38 the water cycle in the hydrological ecosystem (Nie et al., 2014; Yu et al., 2007; Wang et al., 2019)

39 Although the isotopic ratio in soil water varies with depth, it remains stable when transferred from
40 plant roots to stems, leaves or young unbolted branches (Porporato, 2001; Meissner et al., 2014).
41 Precipitation infiltration and runoff generation process (Bam and Ireso, 2018; Hou et al., 2008),
42 groundwater recharge and regeneration capacity (Smith et al., 1992; Cortes and Farvolden, 1989) can
43 be determined combined the isotopic composition changes of surface water, soil water and groundwater.
44 Regional meteorological and hydrological conditions and the contribution of various environmental
45 factors can be evaluated (Hua et al., 2019) by comparing different waterline equations and analyzing
46 changes in various water bodies. Furthermore, it has laid a foundation for studying the deep mechanism
47 of the water cycle (Gao et al., 2009). As an important component of the global water cycle, plants
48 control 50-90% of transpiration (Jasechko et al., 2013; Coenders-Gerrits et al., 2014; Schlesinger and
49 Jasechko, 2014). The plant's roots do not have isotope fractionation when absorbing water (White et al.,
50 1985; Song et al., 2013), so the water isotopic composition of plant roots and stems reflects the isotope
51 composition of water available for plants (Dawson et al., 1991).

52 The research of the water cycle based on SPAC plays a vital role in the study of water and the
53 sources of plant water use in arid areas (Price et al., 2012; Shou et al., 2013). Hydrogen and oxygen
54 isotopes have been used to study the water cycle at the interface of "soil-root", "soil-plant", and
55 "soil-atmosphere", but only a few parameters play an important role in the complex interactions
56 between the various surfaces (Durand et al., 2007; Li et al., 2006; West et al., 2010). Previous studies
57 have shown that local factors, especially temperature, mainly control stable isotope precipitation

58 changes in mid-latitudes (Dai et al., 2020). Through the research on the composition of hydrogen and
59 oxygen isotopes in different water bodies, we can further understand the mechanism of water use by
60 vegetation (Yang et al., 2015) and provide a scientific basis for vegetation restoration in arid and
61 semi-arid areas. In the existing research, how to extend the results of the small-scale SPAC water cycle
62 research to the large-scale area has become a hot and difficult spot. In inland arid areas, due to the lack
63 of water resources, the exchange of energy and water with the outside world is small, and the water
64 cycle is mainly the vertical circulation of groundwater-soil-atmospheric water. Therefore, studying the
65 changes in SPAC isotopic composition in arid regions is significant for ecological restoration.

66 The Shiyang River Basin has the greatest ecological pressure and the most severe water shortage
67 in China. The purpose of this study is to: (1) analyze the SPAC water cycle process in different
68 vegetation zones and (2) identify the potential factors that control the SPAC water cycle. This research
69 is helpful to clarify the water resource utilization mechanism and the local water cycle mechanism of
70 different vegetation areas in high mountainous areas and provide the theoretical basis for the reasonable
71 use of water resources in arid areas.

72 **2 Materials and methods**

73 **2.1 Study area**

74

The Shiyang River Basin is located at the northern foot of the Qilian Mountains, east of the Hexi
75 Region, Gansu Province (Zhu et al., 2018) (Fig. 1). The Shiyang River originates from the
76 snow-capped mountains on the north side of the Lenglongling in the eastern section of the Qilian
77 Mountains. The river's total length is about 250 km, with a basin area of $4.16 \times 10^4 \text{ km}^2$, and the annual
78 average runoff is about $1.58 \times 10^8 \text{ km}^3$. Rivers are supplied by precipitation from mountain and alpine
79 ice and snow melt water. The runoff area is about $1.10 \times 10^4 \text{ km}^2$, and the drought index is 1 to 4 (Zhou
80 et al., 2020). The soil is classified as grey-brown desert soil, aeolian sandy soil, saline soil, and
81 meadow soil. The Shiyang River Basin has a continental temperate arid climate with strong sunlight.
82 The annual average sunshine hours are 2604.8-3081.8 hours, the annual average temperature is
83 $-8.2-10.5^\circ\text{C}$, the temperature difference between day and night is 25.2°C , the annual average

84 precipitation is 222 mm, and the annual average evaporation is 700-2000 mm. The vegetation coverage
85 in the upper and middle alpine regions is better than that of the lower reaches, with trees, shrubs, and
86 grass-covered (Wan et al., 2019). The downstream vegetation coverage is poor under the strong
87 influence of long-term human production, mainly desert vegetation.

88 **Fig 1** about here

89 **2.2 Sample collection**

90 From April 2018 to October 2019, samples were collected at Lenglong (alpine meadow), Hulin
91 (forest), and Xiyang (arid foothills) in the Shiyang River Basin (Table 1). We collected 1281 samples in
92 the Shiyang River Basin, including 472 precipitation samples, 570 soil samples, 119 plant samples, and
93 120 groundwater samples.

94 **Table 1** about here

95 The precipitation samples were collected with a rain bucket. The rain measuring cylinder consists
96 of a funnel and a storage part. After each precipitation event, we immediately transferred the liquid
97 precipitation to a 100 ml high-density sample bottle.. The sample bottle was sealed with a sealing film
98 and stored at low temperature. Simultaneously, the polyethylene bottle sample was labeled with the
99 date and type of precipitation (rain, snow, hail, and rain).

100 The soil samples were collected at intervals of 10 cm at a depth of 100 cm with a soil drill. Part of
101 the soil sample was put into a 50 ml glass bottle. The bottle's mouth was sealed with parafilm and
102 transported to the observation station for cryopreservation within 10 hours after sampling. The
103 remaining soil sample was placed in a 50 ml aluminum box and used the drying method to measure the
104 soil water content (swc).

105 The vegetation samples were collected with a sampling shear. First, we peel off the bark and put
106 the stem into a 50 ml glass bottle. After that, we sealed the bottle mouth and kept it frozen before the
107 experimental analysis.

108 The groundwater samples were collected with polyethylene bottles, and the samples were brought
109 back to the refrigerator at the test station for cryogenic preservation within 10 hours.

110 **2.3 Sample treatment**

111 All water samples were tested using a liquid water analyzer (DLT-100, Los Gatos Research Center,
112 USA) at the Northwest Normal University laboratory. Each sample and isotopic standard werer
113 analyzed by six consecutive injections. To eliminate the memory effect of the analyzer, we discarded
114 the values of the first two injections and used the average of the last four injections as the final result
115 value. Isotopic measurements are given with the symbol "δ" and are expressed as a difference of
116 thousandths relative to Vienna Standard Mean Ocean Water:

$$\delta (\text{‰}) = [(\delta/\delta_{v\text{-smow}}) - 1] \times 1000 \quad (1-1)$$

117 Where, δ is the ratio of ¹⁸O/¹⁶O or ^D/¹H in the collected sample, δ_{v-smow} is the ratio of ¹⁸O/¹⁶O or
118 ^D/¹H in the Vienna standard sample.

119 Due to the existence of methanol and ethanol in plant water samples, it is necessary to calibrate
120 the raw data of plant samples. To determine methanol (NB) and ethanol (BB) pollution degree, we used
121 different concentrations of pure methanol and ethanol mixed deionized water, combined with Los
122 Gatos' LWIA-spectral pollutant identification instrument V1.0 spectral analysis software, and then we
123 established δD and δ¹⁸O spectral pollutant correction method (Meng et al., 2012; Liu et al., 2015). For
124 the broadband metric value NB metric of the methanol calibration result, its logarithm has a significant
125 quadratic curve relationship with ΔδD and Δδ¹⁸O, and the formulas are respectively:

$$\Delta\delta D = 0.018(\ln NB)^3 + 0.092(\ln NB)^2 + 0.388\ln NB + 0.785 \quad (R^2=0.991, p<0.0001) \quad (2-1)$$

$$\Delta\delta^{18}O = 0.017(\ln NB)^3 - 0.017(\ln NB)^2 + 0.545\ln NB + 1.358 \quad (R^2=0.998, p<0.0001) \quad (2-2)$$

126 For ethanol calibration results, the broadband metric value BB metric has a quadratic curve and a
127 linear relationship with ΔδD and Δδ¹⁸O, and the formulas are respectively:

$$\Delta\delta D = -85.67 BB + 93.664 \quad (R^2=0.747, p=0.026) \quad (BB < 1.2) \quad (2-3)$$

$$\Delta\delta^{18}O = -21.421 BB^2 + 39.9356 \quad (R^2=0.769, p<0.012) \quad (2-4)$$

128 **2.4 Data analysis**

129 Since the isotopic data are generally normally distributed according to the Kolmogorov-Smirnov
130 (KS) test, we used Pearson correlation to describe the various correlations between different water
131 types (precipitation, soil water, plant water, and groundwater) and the control factors in different

132 vegetation zones. The significance level for all statistical tests was set to the 95% confidence interval.
133 All statistical analyses completed using the SPSS software.

134 **3. Results**

135 **3.1 Changes in meteorological parameters over time**

136 Figure 2 shows the changes in daily precipitation, relative humidity, temperature, and swc from
137 April 2018 to October 2019. Meteorological data are obtained from the meteorological station in the
138 Shiyang River Basin. During the summer monsoon (April to September), the accumulated precipitation
139 accounts for 90.4% of the total precipitation, and the daily average precipitation is 3.98 mm. During the
140 winter monsoon (October to March), the accumulated precipitation accounts for 9.60% of the total
141 precipitation, with an average daily precipitation of 0.13 mm. During the summer monsoon, the relative
142 humidity of the Shiyang River Basin is 43.78%, while during the winter monsoon it is 35.78%. During
143 the observation period, the temperature is -16.2°C and 32°C , and the average temperature of summer
144 monsoon and winter monsoon are 20.20°C and -0.69°C , respectively. The average SWC value of
145 0-100cm soil layer vary from 2.58% to 89.96 %, and the low SWC value usually appears in summer,
146 which is related to the strong soil evaporation.
147

Fig 2 about here

148 **3.2 The relationship between stable water stable isotopes in different vegetation zones**

149 According to the definition of the global meteoric water line (GMWL) (Craig, 1961), the linear
150 relationship of $\delta^{18}\text{O}$ and δD in local precipitation, soil water, plant water, and groundwater is defined as
151 LMWL, SWL, PWL, and GWL, respectively.

152 As shown in Fig. 3, there are some differences in the local meteoric waterline equations of different
153 vegetation zones. The slope of LMWL of alpine meadows (7.88), forests (7.82), and arid foothills (7.72)
154 is all smaller than that of GMWL (8.00), this is because the study area is located in northwestern
155 China's arid area, where the climate is dry, and the isotopes have undergone strong fractionation. The
156 slope of the SWL in the alpine meadow is the largest (6.07), and the slope of the SWL in the forest
157 (5.10) is greater than the slope of the SWL in the arid foothills (3.94), the intercept has the same
158 characteristics, indicating that the arid foothills' soil evaporation is the largest. According to the Natural
159 Resources Survey Report of the Shiyang River Basin in 2020, the vegetation coverage rate of the alpine
160 meadow is 25.95%, and that of the arid foothills is 8.48%. The vegetation coverage rate of the alpine

161 meadow is higher than that of the arid foothills, and it has better water retention ability and less
162 evaporation of soil water (Wan et al., 2019; Wei et al., 2019). The slope of the PWL in the arid foothills
163 is the largest (2.45), and the slope of the PWL in the alpine meadow (1.90) is greater than that of the
164 forest (1.69).

165 According to the weighted average value of stable oxygen isotopes of various water bodies (Table
166 2), alpine meadows' soil water $\delta^{18}\text{O}$ is -9.16‰, which is the most depleted and the closest to the
167 precipitation $\delta^{18}\text{O}$ (-9.44‰). The average $\delta^{18}\text{O}$ of groundwater is -8.84‰, which is between $\delta^{18}\text{O}$ of
168 plant (-1.68‰) and $\delta^{18}\text{O}$ of precipitation (-9.44‰), indicating that precipitation is the primary source of
169 alpine meadows replenishment. The average $\delta^{18}\text{O}$ of groundwater (-8.56‰) is between soil water $\delta^{18}\text{O}$
170 (-7.01‰) and precipitation $\delta^{18}\text{O}$ (-8.63‰), but it is close to precipitation $\delta^{18}\text{O}$, indicating that forest
171 groundwater is replenished by soil water and precipitation. The mean $\delta^{18}\text{O}$ of soil water (-8.23‰) in
172 the arid foothills are between precipitation $\delta^{18}\text{O}$ (-7.50‰) and groundwater $\delta^{18}\text{O}$ (-8.88‰) but closer to
173 groundwater $\delta^{18}\text{O}$, indicating that the soil water in the arid foothills is mainly supplied by groundwater.
174

175 **Fig 3** about here

Table 2 about here

176 **3.3 Relationship between soil water and plant water isotope in different vegetation zones**

177 By analyzing the isotopic composition of soil and plant xylem, it is possible to preliminarily
178 determine whether there is an overlap between soil moisture and plant moisture at different depths
179 (Javaux et al., 2016; Dawson et al., 1993; Rothfuss et al., 2017; Tetzlaff et al., 2017; McCole et al.,
180 2007; Zhou et al., 2015; Schwendenmann et al., 2015). Soil water may evaporate before being
181 absorbed by plants, which leads to the increase of δD and $\delta^{18}\text{O}$ values of soil water (Chen et al., 2014).
182 Therefore, it can be well explained that the surface soil water isotope in Fig. 4 is more enriched than
183 the deep soil water isotope.

184 According to the study area's precipitation, the current experiment is divided into the dry season
185 (October-April of the following year) and the rainy season (May-September) for analysis (Fig. 4). In
186 the dry season, alpine meadow plants have the highest value of $\delta^{18}\text{O}$ (-2.84‰), and there is no overlap
187 between soil and plant water. In the rainy season, the plant water $\delta^{18}\text{O}$ (-6.04‰) and precipitation $\delta^{18}\text{O}$

188 (-6.40‰) are close, the groundwater and soil water's surface and deep layers intersect, indicating that
189 plant water is mainly supplied by precipitation in the rainy season, while the groundwater is supplied
190 by soil water. In the dry season, due to the low temperature (average temperature 0.30°C), there is a lot
191 of ice and snow in alpine meadows, and plants do not directly use soil water. As the increase of
192 temperature (average temperature 8.72°C), precipitation and surface runoff increases, and water
193 infiltrate groundwater from soil. Forest plant water intersects with deep soil during the dry season and
194 intersects with the soil surface during the rainy season, indicating that forest plants mainly use deep soil
195 water during the dry season and shallow soil water during the rainy season. In the rainy season, the
196 surface layer of soil water intersects with plant water, the groundwater and soil water's surface and
197 deep layers intersect, showing that the plant water preferentially uses the surface layer water of the soil
198 in the arid foothills. In the dry season, plant water oxygen is the most enriched, and the isotopic values
199 of groundwater and soil water are close, indicating that the soil water is mainly recharged by the
200 groundwater. According to the Natural Resources Survey Report of the Shiyang River Basin, the buried
201 groundwater level in the arid foothills is 2.5-15 m, and the groundwater table is relatively shallow,
202 making the soil water in the arid foothills mainly recharged by groundwater in the dry season.

203

Fig 4 about here

204 **4. Discussion**

205 **4.1 Variation of soil water isotope and SWC between different vegetation zones**

206 In Fig. 5, along the three vegetation zones of alpine meadow-forest-arid foothills, soil water
207 isotope is gradually enriched. The coefficient of variation of the arid foothills is the largest (-0.15),
208 while that of the forest is the smallest (-0.25), indicating that from forest to arid foothills, the closer to
209 arid regions, the greater the coefficient of variation and that the greater the instability of soil water
210 isotope. The soil water isotopes of different vegetation zones showed the same characteristics as the
211 soil depth changed, that is, they were all depleted in May and August and enriched in October.

212 The swc of alpine meadows (average θ of 42.21%) is higher than that of forests (average θ of
213 26.98%) and arid foothills (average θ of 17.05%), and the swc of alpine meadows increases with the
214 increase of soil depth (from 43.78%to 49.27%), while that of forests the swc decreases with the soil
215 depth (from 26.10%to 25.41%). Compared with forests, plants in alpine meadows have shallower root
216 systems and smaller canopies, so transpiration and water consumption are lower, and swc is higher
217 (Csilla et al., 2014; Li et al., 2009; Western et al., 1998). On the one hand, with the improvement of
218 vegetation restoration, the ability of alpine meadows to retain soil water has enhanced, and the soil
219 water evaporation has reduced On the other hand, Lenglong, a representative of alpine meadows, has
220 an average annual precipitation of 595.10 mm, and a low temperature (average annual temperature of
221 -0.20°C), makes the soil water evaporation intensity weak. The swc of the alpine meadows (86.95%)
222 and forests (53.45%) is the largest in August, while the arid foothills' swc (11.13%) is the smallest in
223 August, this is because the northern slope of the Qilian Mountains is a windward slope. In August, a lot
224 of precipitation falls on the high-altitude alpine meadows and forests, the arid foothills have little
225 precipitation and low swc.
226

Fig 5 about here

227 4.2 Control factors of SPAC in different vegetation zones

228 4.2.1 The influence of temperature on SPAC

229

230 As shown in Fig. 6, with the changes in the water cycle of precipitation-soil water-plant water, the
231 $\delta^{18}\text{O}$ of forests gradually enriched, while the soil water $\delta^{18}\text{O}$ of arid foothills and alpine meadows are
232 the most depleted in summer. In other seasons, $\delta^{18}\text{O}$ is gradually enriched along with precipitation-soil
233 water-plant water. In summer, there is much precipitation and large swc in alpine meadows, but due to
234 the low temperature (average temperature in summer is 9.80°C), the soil water $\delta^{18}\text{O}$ of alpine meadows
235 is relatively depleted. In the arid foothills, in summer, especially in August, although the temperature is
236 relatively high (the average temperature is 23.92°C), the swc is low, evaporation is weak, and $\delta^{18}\text{O}$ are
237 relatively depleted. This phenomenon shows that precipitation plays a major control role in the water
cycle of precipitation-soil-plants. When the temperature is below 0°C , the air will expand adiabatically,

238 and the water vapor will change adiabatic cooling (Rozanski, 1992). When the temperature is between
239 0°C and 8°C, the influence of local water vapor circulation is greater. When the temperature is below
240 8°C, the below-cloud evaporation is very strong (Zhu et al., 2021). Therefore, we divided the
241 temperature into three gradients (below 0°C, between 0°C and 8°C and above 8°C) for analysis. From
242 the alpine meadow to arid foothills, the correlations between temperature and soil $\delta^{18}\text{O}$ are 0.41, 0.30,
243 and 0.19, respectively, and the correlations with plant $\delta^{18}\text{O}$ are 0.24, 0.27, and 0.25, respectively, and
244 the temperature effect is not significant compared with precipitation. As shown in Table 3, from the
245 alpine meadow to the arid foothills, the temperature effect of the precipitation isotope increased, and
246 there is a significant positive correlation with temperature and all of which have passed the significance
247 test. With the increase of temperature, the linear relationship between temperature and precipitation
248 isotope in each vegetation zone became weaker. When the temperature is lower than 0°C, the
249 correlation between precipitation $\delta^{18}\text{O}$ and the temperature in the arid foothills fails to pass the
250 significance test.. The relationship between $\delta^{18}\text{O}$ and temperature in alpine meadows, forests, and arid
251 foothills are $\delta^{18}\text{O}=0.62T-10.84$, $\delta^{18}\text{O}=1.58T-12.14$, and $\delta^{18}\text{O}=1.29T-11.78$, respectively. When the
252 temperature is between 0°C and 8°C, the temperature effect of precipitation weakens with the
253 temperature increases,, which may be related to the weakening of the local water cycle and the
254 enrichment of precipitation isotopes. The relationship between $\delta^{18}\text{O}$ and temperature in alpine
255 meadows, forests, and arid foothills are $\delta^{18}\text{O}=0.51T-11.41$, $\delta^{18}\text{O}=2.46T-22.84$, and $\delta^{18}\text{O}=2.27T-22.78$,
256 respectively. When the temperature is above 8°C, there is no correlation between the precipitation $\delta^{18}\text{O}$
257 and the temperature, but the precipitation $\delta^{18}\text{O}$ is the most enriched, which may be related to the $\delta^{18}\text{O}$
258 enrichment caused by the below-cloud evaporation. The relationship between $\delta^{18}\text{O}$ and temperature in

259 alpine meadows, forests, and arid foothills are $\delta^{18}\text{O}=0.48T-10.82$, $\delta^{18}\text{O}=0.13T-7.76$, and
260 $\delta^{18}\text{O}=0.27T-10.13$, respectively.

261 **Fig 6** about here

262 **Table 3** about here

263 **4.2.2 The influence of altitude on SPAC**

264 In Fig.7, the altitude effect of precipitation $\delta^{18}\text{O}$ is the strongest, and the relationship between
265 plant water $\delta^{18}\text{O}$ and altitude is weakest, showing that in SPAC, precipitation isotope is most affected
266 by altitude, and plant water isotope is least affected by altitude. From the arid foothills to alpine
267 meadows, the elevation increases from 2097m to 3647m, and the change rate of $\delta^{18}\text{O}$ and δD was
268 $-0.11\text{‰} (100\text{m})^{-1}$ and $-0.41\text{‰} (100\text{m})^{-1}$. As the water vapor quality increases along the hillside, the
269 temperature continues to decrease, and the isotopic values of precipitation continue to consume. In the
270 rainy season, the squares of the correlation coefficients between precipitation $\delta^{18}\text{O}$ and altitude,
271 precipitation δD and altitude are 0.79 and 0.98, the change rate of $\delta^{18}\text{O}$ and δD are $-0.12\text{‰} (100\text{m})^{-1}$
272 and $-1.05\text{‰} (100\text{m})^{-1}$, respectively. In the dry season, the correlation coefficient squares between
273 precipitation $\delta^{18}\text{O}$ and altitude, precipitation δD and altitude are 0.88 and 0.90, respectively, and the
274 rate of $\delta^{18}\text{O}$ and δD change is $-0.18\text{‰} (100\text{m})^{-1}$ and $-0.79\text{‰} (100\text{m})^{-1}$, respectively. We can see that the
275 altitude effect of precipitation $\delta^{18}\text{O}$ is stronger in the dry season ($R^2=0.88$) than in the rainy season
276 ($R^2=0.79$). The results showed that as the temperature increase, the temperature effect of precipitation
277 $\delta^{18}\text{O}$ masks the altitude effect, which leads to the weakening of the altitude effect of precipitation $\delta^{18}\text{O}$.
278 The relationship between soil water $\delta^{18}\text{O}$ and altitude is stronger in the dry season ($R^2=0.26$) than in the
279 rain season ($R^2=0.28$). The relationship between plant water $\delta^{18}\text{O}$ and altitude is stronger in the dry
280 season ($R^2=0.11$) than in the rainy season ($R^2=0.10$), this is consistent with the changes in the altitude

281 effect of precipitation isotope .

282 **Fig 7** about here

283 **4.2.3 The influence of relative humidity and precipitation on SPAC**

284 To find out the potential factors that control the isotope composition of SPAC in different
285 vegetation zones, we also analyzed the influence of relative humidity and precipitation on $\delta^{18}\text{O}$ of
286 SPAC. It can be seen from Fig. 8 and Table 4 that the greatest impact of relative humidity on the
287 isotope composition of SPAC appears in the arid foothills in the dry season, with a correlation
288 coefficient of 0.38. Although in the dry season, the square of the correlation coefficient between forest
289 precipitation isotope and relative humidity is 0.78, there is an inverse humidity relationship between
290 the two, which may be related to the lack of precipitation samples in the dry season. The largest impact
291 of precipitation on the isotopic composition of SPAC occurs in the arid foothills in the rainy season,
292 and the square of the correlation coefficient is 0.14. It can also be seen from Fig. 8 that the influence of
293 relative humidity and precipitation on precipitation isotope is greater than that on plant water isotope
294 and soil water isotope. The influence of relative humidity and precipitation on the isotopic composition
295 of SPAC in alpine meadows is greater than that in arid foothills and greater than that in forests. The
296 influence of relative humidity and precipitation on the isotopic composition of SPAC in alpine
297 meadows is greater than that of arid foothills and greater than that of forests. In general, the SPAC
298 isotopic composition of alpine meadows, forests, and arid foothills has a weak precipitation effect, and
299 the correlation with relative humidity is also weak.

300 By comparing the correlation of temperature, altitude, relative humidity and precipitation with
301 SPAC isotope composition in different vegetation zones, we can see that the correlation between
302 temperature and altitude and SPAC isotope composition is stronger than relative humidity and

303

precipitation. Temperature and altitude are potential factors that control the isotope composition of
304 SPAC. However, in the dry season, there is a phenomenon that the temperature effect conceals the
305 altitude effect.

306

Fig 8 about here

307

Table 4 about here

308 **5. Conclusion**

309 This paper uses the hydrogen and oxygen isotope method to study the differences and control
310 factors of SPAC in different vegetation zones. Temperature and altitude are the main control factors for
311 the isotopic composition of SPAC.. From alpine meadows to forests to arid foothills, as the decreases
312 of altitude, the temperature effect of precipitation isotope increases, and the influence of temperature
313 also increases. When the temperature is lower than 0°C, the temperature effect of the vegetation zone is
314 the strongest. In the dry season, there is a phenomenon that the temperature effect masks the altitude
315 effect. With the increase of the soil depth, the soil water isotopes are gradually depleted. The soil water
316 content of alpine meadows is the largest and increases with the soil depth, while the soil water content
317 in forest decreases with the soil depth, and the soil water content of the arid foothills is the least in
318 August. In the rainy season, plants mainly use precipitation, while forest plants mainly use soil water in
319 the dry season. Alpine meadow plants do not directly use soil water because of the abundant
320 precipitation and melt water in the growing season. The groundwater table exposed in the arid foothills
321 can provide water for plants in the dry season. Forests and grasslands affect intercepting rainfall, they
322 delay or hinder the formation of surface runoff and convert part of the surface runoff into soil flow and
323 groundwater, which can provide part of water resources for plants. To better understand the water cycle
324 of SPAC at different temperatures and altitudes in high mountain areas, long-term observations of
325 different plants are needed to provide a theoretical basis for the rational and practical use of water
326 resources in arid mountainous areas.

327 **Data Availability**

328 The data that support the findings of this study are openly available in Zhu (2021), "Stable
329 water isotope monitoring network of different water bodies in Shiyang River Basin, a typical arid
330 river in China (Supplemental Edition 20210808)", Mendeley Data, V1, doi:

331 10.17632/d5kzm92nn3.1.

332 **Author contribution**

333 Guofeng Zhu and Yuwei Liu conceived the idea of the study; Zhuanxia Zhang analyzed the data;
334 Zhigang Sun and Leilei Yong were responsible for field sampling; Liyuan Sang participated in the
335 experiment; Kailiang Zhao participated in the drawing; Yuwei Liu wrote the paper; Liyuan Sang and
336 Lei Wang checked and edited language. All authors discussed the results and revised the manuscript.

337 **Competing interests**

338 The authors declare no competing interests

339 **Acknowledgments**

340 This research was financially supported by the National Natural Science Foundation of China
341 (41661005, 41867030, 41971036). The authors much thank the colleagues in the Northwest Normal
342 University for their help in fieldwork, laboratory analysis, data processing.

343 **References**

344 Araguás-Araguás, L, Froehlich, K., and Rozanski, K.: Stable isotope composition of precipitation over
345 southeast asia. *Journal of Geophysical Research Atmospheres*, 103 (D22), 28721-28742, doi:
346 10.1029/98JD02582,1998.

347 Bam, E., and Ireson, A. M.: Quantifying the wetland water balance: a new isotope-based approach that
348 includes precipitation and infiltration. *Journal of Hydrology*, 570, doi:
349 10.1016/j.jhydrol.2018.12.032, 2018.

350 Chen, X. L., Chen, Y. N., and Chen, Y. N P.: Water use relationship of desert riparian forest in lower
351 reaches of Heihe River. *Chinese Journal of Eco-Agriculture*, 22 (08):972-979,
352 doi:10.1007/s11430-013-4680-8, 2014.

353 Christopher, T., Solomon, J, J., and Cole.: The influence of environmental water on the hydrogen stable
354 isotope ratio in aquatic consumers. *Oecologia*, 161 (2), p.313-324, doi:
355 10.1007/s00442-009-1370-5, 2009.

356 Coenders-Gerrits, A. M, J., van der Ent, R.J., Bogaard, T. A., Wang-Erlandsson, L., Hrachowitz, M.,
357 Savenije, and H. H. G.: Uncertainties in transpiration estimates. *Nature*. 506, E1–E2, doi:
358 10.1038/nature12925, 2014.

359 Coplen, T.: Stable isotope hydrology: deuterium and oxygen 18 in the water cycle. *Eos Transactions*
360 *American Geophysical Union*, 63 (45), 861-862, doi: 10.1029/EO063i045p00861, 2013.

361 Cortes, A., and Farvolden, R. N.: Isotope studied of precipitation and groundwater in the sierra de las
362 cruces, Mexico. *Journal of Hydrology*, 107 (1–4), 147-153, doi:
363 10.1016/0022-1694(89)90055-3,1989.

364 Craig, H.: Isotopic variations in meteoric water. *Science*, 133, 1702–1703, doi:
365 10.1126/science.133.3465.1702,1961.

366 Csilla, F., Györgyi, G., Zsófia, B., and Eszter, T.: Impact of expected climate change on soil water
367 regime under different vegetation conditions. *Biologia*, doi: 10.2478/s11756-014-0463-8, 2014.

368 Dai, J. J., Zhang, X. P., Luo, Z. D., Wang, R., Liu, Z. L., He, X. G., and Guan, H. D.: Variation of the
369 stable isotopes of water in the soil-plant-atmosphere continuum of a *Cinnamomum camphora*
370 woodland in the East Asian monsoon region. *Journal of Hydrology*, 589, 125199. doi:
371 10.1016/J.JHYDROL.2020.1251, 2020.

372 Darling, W. G. , Bath, A. H. , and Talbot, J. C.: The O and H stable isotope composition of freshwaters
373 in the british isles. 2, surface waters and groundwater. *Hydrology and Earth System Sciences*, doi:
374 10.5194/hess-7-183-2003, 2003.

375 Dawson, T. E., and Ehleringer, J. R.: Streamside trees that do not use stream water. *Nature*, 350 (6316),
376 335-337, doi: 10.1038/350335a0, 1991.

377 Dawson, T. E.: Water sources of plants as determined from xylem-water isotopic composition:
378 perspectives on plant competition, distribution, and water relations stable isotopes and plant
379 carbon water relations. *Stable Isotopes and Plant Carbon-water Relations*, 465-496, 1993.

380 Detjen, M., Sterling, E. , and Gómez, A.: Stable isotopes in barnacles as a tool to understand green sea
381 turtle (*Chelonia mydas*) regional movement patterns. *Biogeosciences*, 2015.

382 Durand, J. L., Bariac, T., M Ghesquière, Biron, P., Richard, P., and Humphreys, M.: Ranking of the
383 depth of water extraction by individual grass plants, using natural ¹⁸O isotope
384 abundance. *Environmental and Experimental Botany*, 60 (1), 137-144, doi:
385 10.1016/j.envexpbot.2006.09.004, 2007.

386 Ehleringer, L.: Stable isotope composition of stem and leaf water: applications to the study of plant
387 water use. *Functional Ecology*, 5 (2), 270-277, doi:10.2307/2389264,1991.

388 Gao, J., Tian, L. D., Liu, Y. Q., and Gong, T. L.: Oxygen isotope variation in the water cycle of the
389 Yamzho lake basin in southern Tibetan plateau. *Chinese Science Bulletin*, (16), 2758-2765, 2009.

390 Gao, J., Yao, T., Tian, L.D., Risi, C., and Hoffmann, G.: Precipitation water stable isotopes in the south

391 tibetan plateau: observations and modeling. *Journal of Climate*, 24 (13), 3161-3178, doi:
392 10.1175/2010JCLI3736.1, 2011.

393 Hou, S. B., Song, X. F., Jie, Y. J., Liu, X., and Zhang, G. Y.: Stable isotopes characters in the process of
394 precipitation and infiltration in taihang mountainous region. *Resources Science*, 2008.

395 Hua, M. Q., Zhang, X. P., Yao, T. C., and He, X. G.: Dual effects of precipitation and evaporation on
396 lake water stable isotope composition in the monsoon region. *Hydrological Processes*, 33,
397 2192–2205, doi: 10.1002/hyp.13462, 2019.

398 Jasechko, S., Sharp, Z. D., Gibson, J. J., Birkes, S. J., Yi, Y., and Fawcett, P. J.: Terrestrial water fluxes
399 dominated by transpiration. *Nature*, 496 (7445), 347–351, doi: 10.1038/nature11983, 2013.

400 Javaux, M., Rothfuss, Y., Vanderborght, J., Vereecken, H., and Brüggemann, N.: Isotopic composition
401 of plant water sources. *Nature*, 536 (7617), E1–E3, doi: 10.1038/nature18946, 2016.

402 Li, C. C., Huang, M. S., Liu, J., Ji, S. P., and Zhao, R. Q.: Isotope-based water-use efficiency of major
403 greening plants in a sponge city in northern China. *PloS one*, 14 (7), doi:
404 10.1371/journal.pone.0220083, 2019.

405 Li, L. F., Yan, J. P., Liu, D. M., Chen, F., and Ding, J. M.: Changes in soil water content under different
406 vegetation conditions in arid-semi-arid areas and analysis of vegetation construction methods.
407 *Bulletin of Soil and Water Conservation*, 29 (001), 18-22, 2009.

408 Li, S. G., Maki, T., Atsuko, S., and Michiaki, S.: Seasonal variation in oxygen isotope composition of
409 waters for a montane larch forest in Mongolia. *Trees* (1), doi: 10.1007/s00468-005-0019-1, 2006.

410 Liu, W., Wang, P., Li, J., Liu, W., and Li, H.: Plasticity of source-water acquisition in epiphytic,
411 transitional and terrestrial growth phases of *Ficus tinctoria*. *Ecohydrology*, 7 (6), 1524–1533, doi:
412 10.1002/eco.1475, 2015.

413 McCole, A. A., and Stern, L. A.: Seasonal water use patterns of *Juniperus ashei* on the Edwards Plateau,
414 Texas, based on stable isotopes in water. *Journal of Hydrology*, 342, 238–248, doi:
415 10.1016/j.jhydrol.2007.05.024, 2007.

416 Meissner, K., Schwendenmann, H., and Dyckmans.: Soil water uptake by trees using water stable
417 isotopes (δD and $\delta^{18}O$)- a method test regarding soil moisture, texture and carbonate. *Plant*
418 *Soil*, 376, 327-335, doi: 10.1007/s11104-013-1970-z, 2014.

419 Meng, X. Q., Wen, X. F., Zhang, X. Y., Han, J. Y., Sun, X. M., and Li, X. B.: Influence of organics on
420 the determination of $\delta^{18}O$ and δD of plant leaves and stalk water by infrared spectroscopy, *Chin J*

421 Eco-agri, 20, 1359-1365, 2012.

422 Nie, Y. P., Chen, H. S., Wang, K. L., and Ding, Y. L.: Rooting characteristics of two widely distributed
423 woody plant species growing in different karst habitats of southwest China. *Plant Ecol*, 215
424 (10),1099-1109, doi: 10.1007/s11258-014-0369-0, 2014.

425 Nlend, B., Celle-Jeanton, H., Risi, C., Pohl, B., and Ketchemen-Tandia, B.: Identification of processes
426 that control the stable isotope composition of rainwater in the humid tropical west-central
427 Africa. *Journal of Hydrology*, 584, 124650, doi:10.1016/j.jhydrol.2020.124650, 2020.

428 Porporato, L.: Plants in water-controlled ecosystems: active role in hydrologic processes and response
429 to water stress. *Advances in Water Resources*, 24 (7), 725-744, doi:
430 10.1016/S0309-1708(01)00005-7, 2001.

431 Price, R. M., Skrzypek, G., Grierson, P. F., Swart, P. K., and Fourqurean, J. W.: The use of stable
432 isotopes of oxygen and hydrogen to identify water sources in two hypersaline estuaries with
433 different hydrologic regimes. *Marine and Freshwater Research*, 63 (11), 952-966. doi:
434 10.1071/MF12042, 2012.

435 Raco, B., Dotsika, E., Feroni, A. C., Battaglini, R., and Poutoukis, D.: Stable isotope composition of
436 italian bottled waters. *Journal of Geochemical Exploration*, 124, doi:
437 10.1016/j.gexplo.2012.10.003, 2013.

438 Rothfuss, Y., and Javaux, M.: Reviews and syntheses: Isotopic approaches to quantify root water
439 uptake: A review and comparison of methods. *Biogeosciences*, 14, 2199,
440 doi:10.5194/bg-14-2199-2017, 2017.

441 Rozanski, K., Araguas-Araguas, L., and Gonfiantini, R.: Relation between long-term trends of
442 oxygen-18 isotope composition of precipitation and climate. *Science* 258 (5084), 981–985, doi:
443 10.1126/science.258.5084.981, 1992.

444 Schlesinger, W. H., and Jasechko, S.: Transpiration in the global water cycle. *Agric Forest Meteorol*,
445 180–190, 115–117, doi: 10.1016/j.agrformet.2014.01.011, 2014.

446 Schwendenmann, L., Pendall, E., Sanchez-Bragado, R., Kunert, N., Hölscher, D.: Tree water uptake in
447 a tropical plantation varying in tree diversity: Interspecific differences, seasonal shifts and
448 complementarity. *Ecohydrology*, 8 (1), 1–12, doi: 10.1002/eco.1479, 2015.

449 Shou, W. K., Hu, F. L., Alamusa., and Liu, Z. M.: Methods for studying water cycle and water sources
450 in arid regions based on spac system. *Chinese Journal of Ecology*, 32 (8), 2194-2202, 2013.

451 Smith, G. I., Friedman, I., Gleason, J. D., and Warden, A.: Stable isotope composition of waters in
452 southeastern California: 2. groundwaters and their relation to modern precipitation. *Journal of*
453 *Geophysical Research Atmospheres*, 97, doi: 10.1029/92JD00183,1992.

454 Song, X. F., Xia, J., Yu, J. J., and Liu, C. M.: Application of environmental isotope techniques to study
455 the hydrological cycle mechanism of typical watersheds in North China. *Advances in*
456 *Geographical Sciences*, 21 (6), 527-537, 2002.

457 Song, X., Barbour, M. M., Farquhar, G. D., Vann, D. R., and Helliker, B. R.: Transpiration rate relates
458 to within and across species variations in effective path length in a leaf water model of oxygen
459 isotope enrichment. *Plant, Cell and Environment*, 36 (7), 2013.

460 Sun, S. F., Huang, J. H., Lin, G. H., Zhao, W., and Han, X. G.: Application of stable isotope technique
461 in the study of plant water use. *Acta Ecologica Sinica*, 25 (9), 2362-2371. Tech. Pap, No. 96 (48
462 pp.), doi: 10.1360/982004-755, 2005.

463 Tetzlaff, D., Sprenger, M., and Soulsby, C.: Soil water stable isotopes reveal evaporation dynamics at
464 the soil-plant-atmosphere interface of the critical zone. *Hydrol. Earth Syst. Sci*, 21, 3839–3858,
465 2017.

466 Wan, Q. Z., Zhu, G. F., Guo, H. W., Zhang, Y., Pan, H. X., and Yong, L. L.: Influence of vegetation
467 coverage and climate environment on soil organic carbon in the Qilian mountains. *Scientific*
468 *Reports*, 9(1), 17623. doi: 10.1038/s41598-019-53837-4, 2019.

469 Wang, S. Y., Wang, Q. L., Wu, J. K., He, X. B., and Wang, L. H.: Characteristics of stable isotopes in
470 precipitation and moisture sources in the headwaters of the Yangtze River. *Environmental*
471 *Sciences*, 40 (6), 2615-2623, doi: 10.13227/j.hjxk.201811140, 2019.

472 West, A. G., Patrickson, S. J., and Ehleringer, J. R. : Water extraction times for plant and soil materials
473 used in stable isotope analysis. *Rapid Communications in Mass Spectrometry*, 20 (8), 1317-1321.
474 doi: 10.1002/rcm.2456, 2010.

475 Western, A. W., and Grayson, R. B.: The tarrawarra data set: soil moisture patterns, soil characteristics,
476 and hydrological flux measurements. *Water Resources Research*, 34 (10), 2765-2768. doi:
477 10.1029/98WR01833, 1998.

478 White, J., Cook, E., Lawrence, J. R., and Broecker, W. S.: The D/H ratios of sap in trees: implications
479 for water sources and tree ring D/H ratios. *Geochim. Cosmochim. Acta*, 49 (1), 237–246, doi:
480 10.1016/0016-7037(85)90207-8,1985.

481 Yang, B., Wen, X., and Sun, X.: Seasonal variations in depth of water uptake for a subtropical
482 coniferous plantation subjected to drought in an east asian monsoon region. *Agricultural and*
483 *Forest Meteorology*, 201, 218-228, doi: 10.1016/j.agrformet.2014.11.020, 2015.

484 Yu, J. J., Song, X. F., Liu, X. C., Yang, C., Tang, C. Y., and Li, F. D.: A study of groundwater cycle in
485 yongding river basin by using δD , $\delta^{18}O$ and hydrochemical data. *Journal of Natural Resources*,
486 (03), 415-423, 2007.

487 Zhou, H., Zhao, W. Z., Zheng, X. J., and Li, S. J.: Root distribution of *Nitraria sibirica* with seasonally
488 varying water sources in a desert habitat. *J. Plant Res*, 128, 613–622, 2015.

489 Zhou, J. J., Zhao, Y. R., Huang, P., and Liu, C. F.: Impacts of ecological restoration projects on the
490 ecosystem carbon storage of inland river basin in arid area, China. *Ecological Indicators*, doi:
491 10.1016/j.ecolind.2020.106803, 2020.

492 Zhu, G. F., Guo, H.W., Qin, D. H., Pan, H. X., and Ma, X. G.: Contribution of recycled moisture to
493 precipitation in the monsoon marginal zone: estimate based on stable isotope data. *Journal of*
494 *Hydrology*, 569, doi: 10.1016/j.jhydrol.2018.12.014, 2018.

495 Zhu, G. F., Zhang, Z. X., Guo H. W., Zhang, Y., Yong, L. L., Wan, Q. Z., Sun, Z. G., and Ma, H.Y.:
496 Below-Cloud Evaporation of Precipitation Isotope over Mountain-oasis-desert in Arid Area. *Journ*
497 *al of Hydrometeorology*, 22 (10): 2533-2545, doi: 10.1175/JHM-D-20-0170.1, 2021.

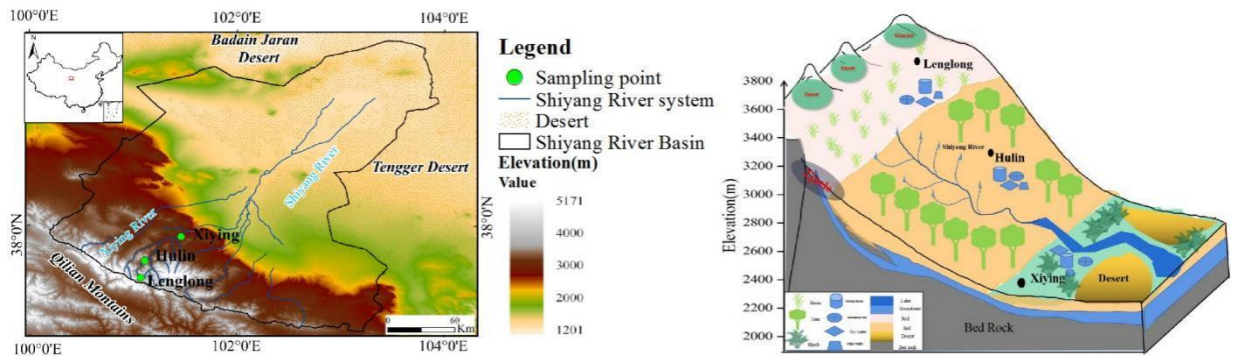


Fig. 1 Study area and observation system

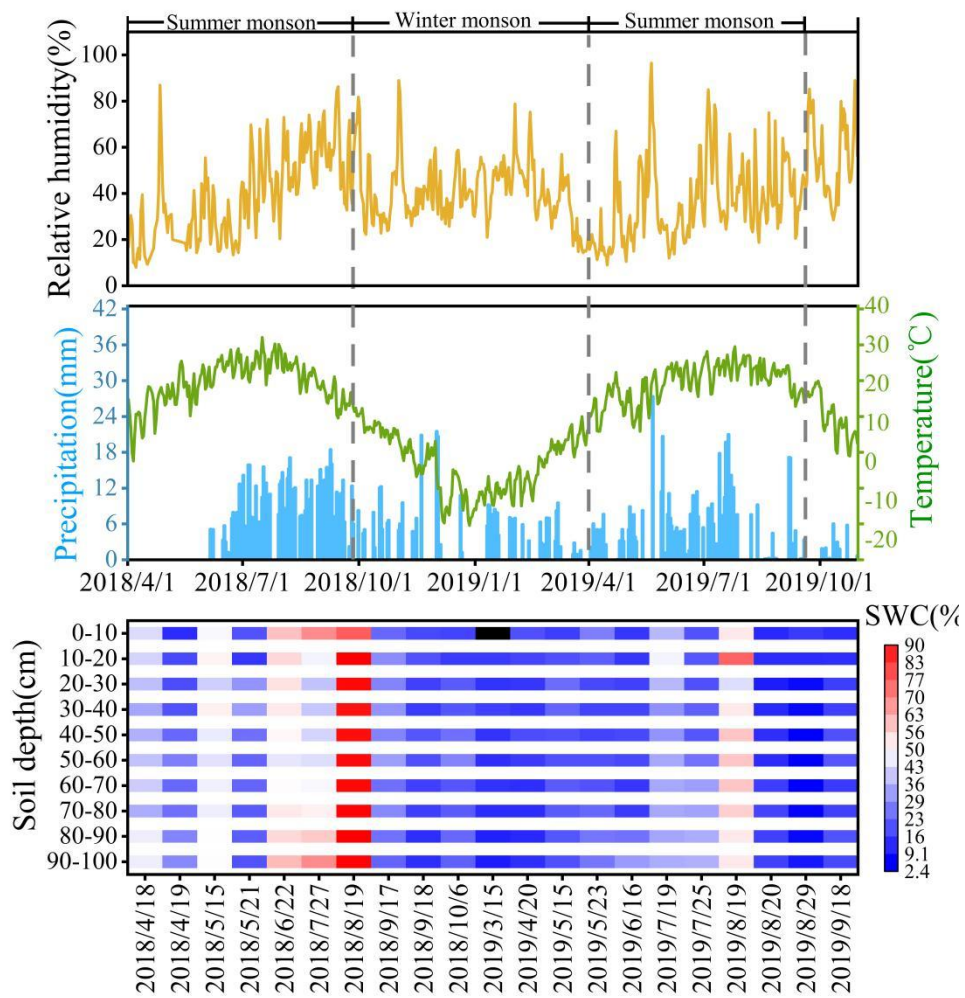


Fig. 2 Diurnal variation of relative humidity, precipitation, temperature, and swc (%) from April 2018 to October 2019

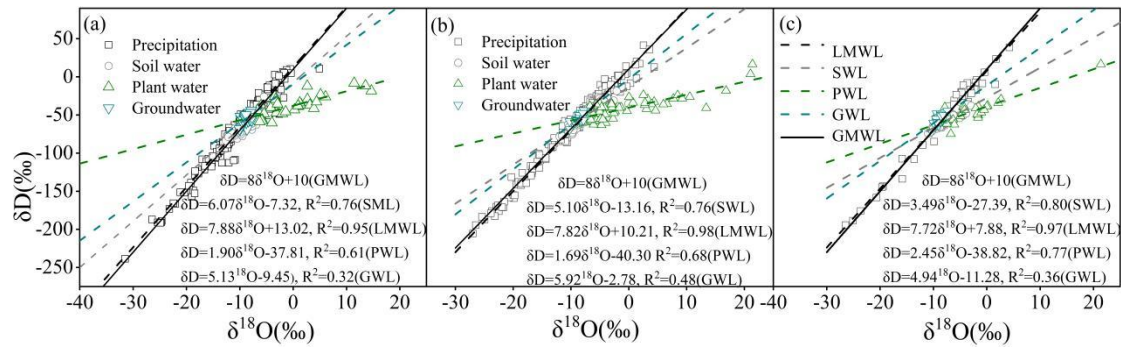


Fig.3 Relationship of stable isotopes in different water bodies in alpine meadow (a), forest (b) and arid foothills (c)

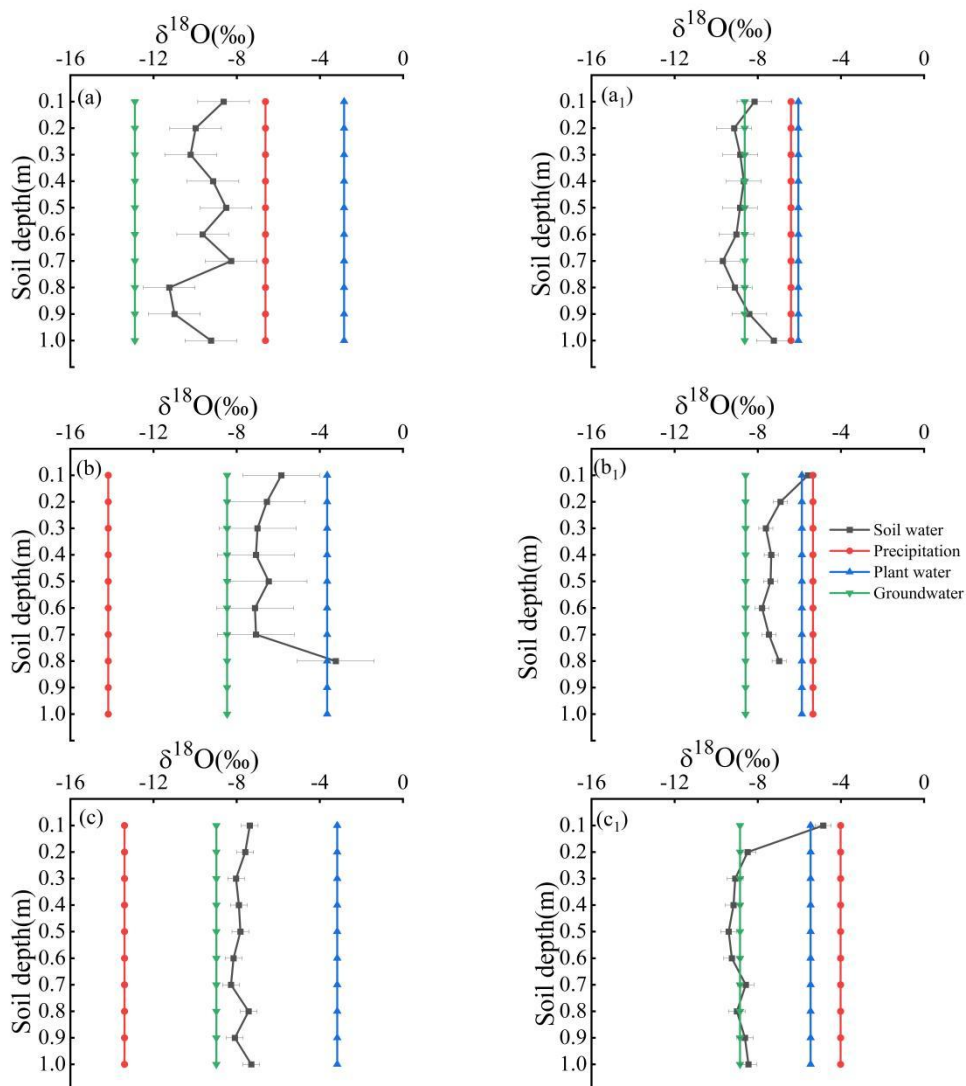


Fig. 4 (a)-(c) represents the variation of $\delta^{18}O$ of soil, plant, precipitation and groundwater with soil depth in the alpine meadow, forests and arid foothills in the dry season, and (a₁)-(d₁) represents the variation of $\delta^{18}O$ of soil, plant, precipitation and groundwater in the alpine meadow, forests and arid foothills in the rainy season

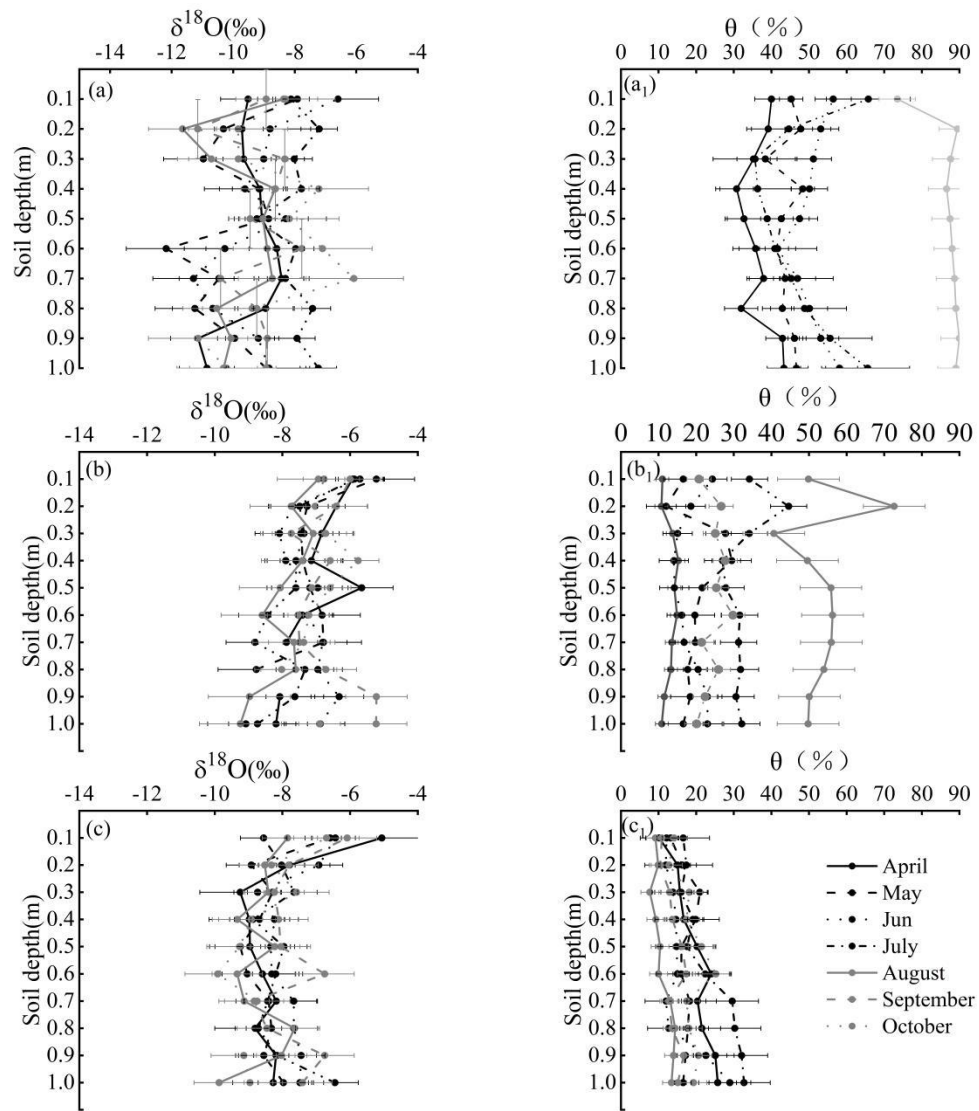


Fig.5 The variation of $\delta^{18}\text{O}$ and soil water content (θ , %) with soil depth. (a)-(c) represent alpine meadow, forests and arid foothills, respectively

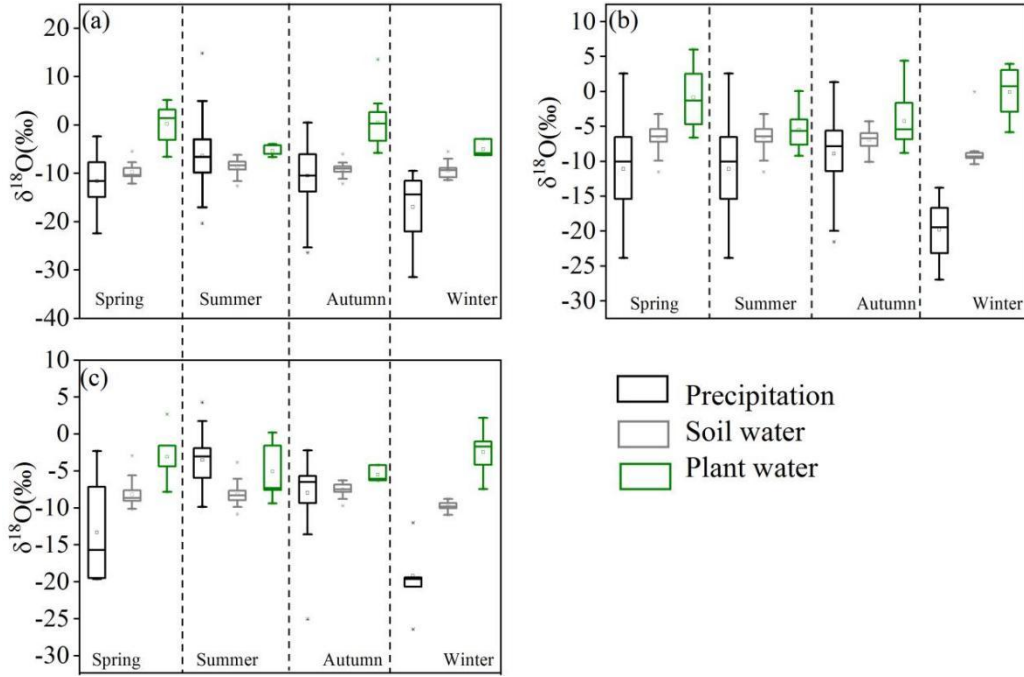


Fig. 6 Seasonal variations of different water isotopes in alpine meadow (a), forests (b) and arid foothills (c)

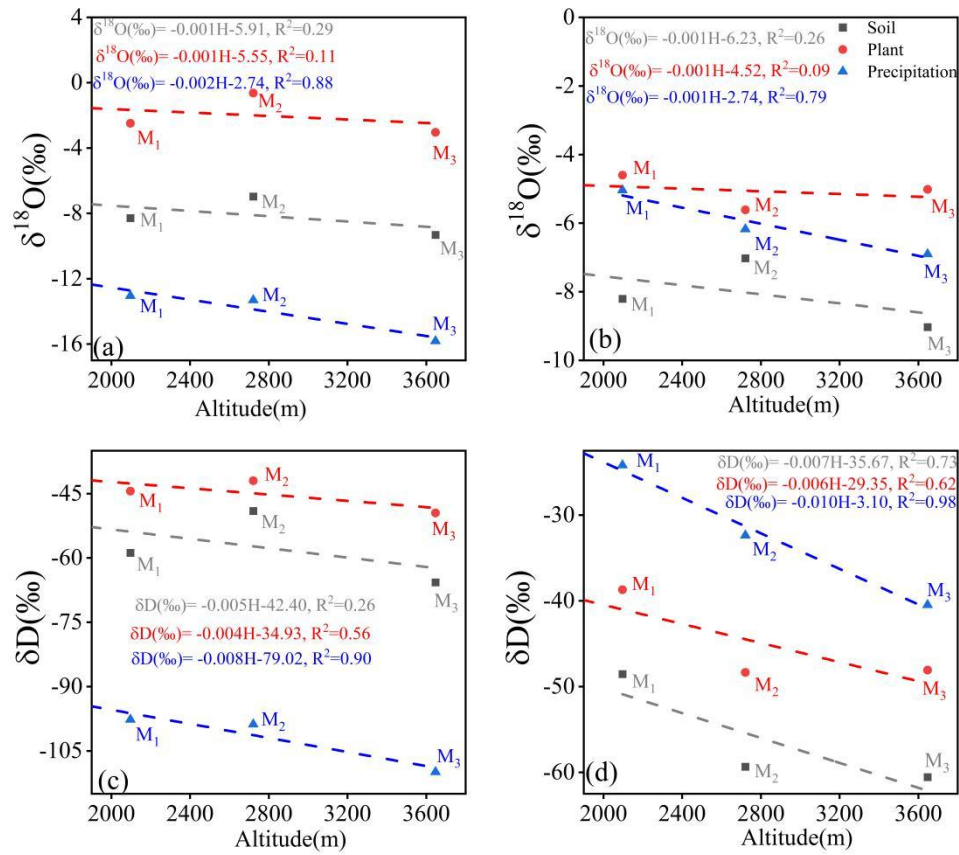


Fig. 7 Relationship between different isotope and altitude in the dry season (a, c) and in the rain season (b, d), M₁ stands for alpine meadows, M₂ stands for forests, and M₃ stands for arid foothills

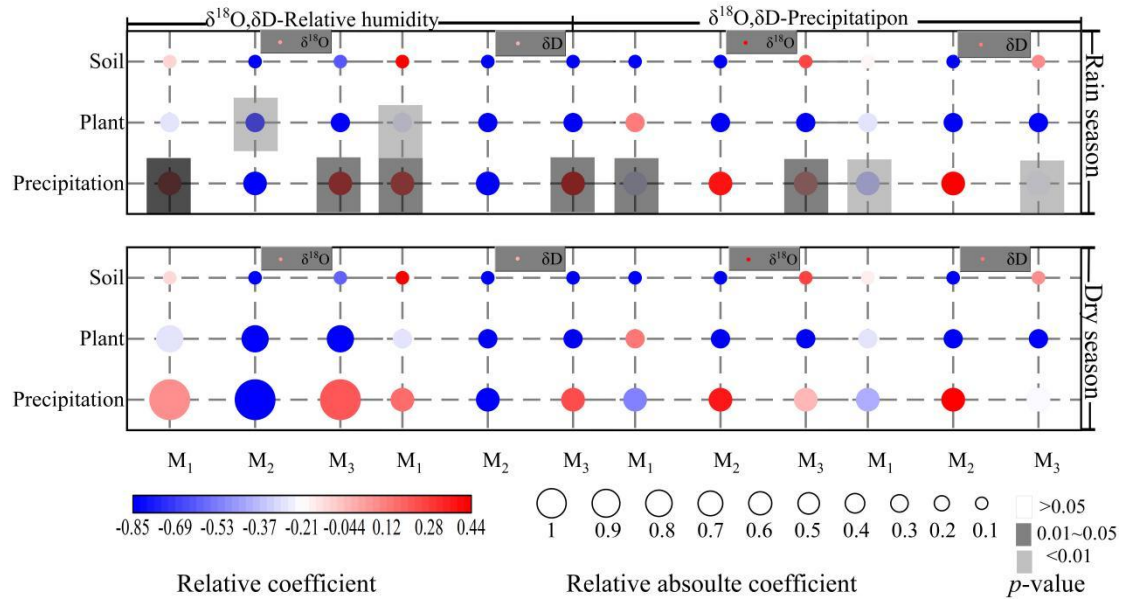


Fig. 8 Relationship between different isotope and relative humidity and precipitation, M₁ stands for alpine meadows, M₂ stands for forests, and M₃ stands for arid foothills

Table 1 Basic information table of sampling points

Sampling Station		Geographical Parameters			Meteorological Parameters	
		Longitude (E)	Latitude (N)	Altitude (m)	Average annual temperature (°C)	Average annual precipitation (mm)
M1	Lenglong	101°50'	37°33'	3647	-0.20	595.10
M2	Hulin	101°53'	37°41'	2721	3.24	469.44
M3	Xiyang	102°18'	38°29'	2097	7.99	194.67

Table 2 Comparison of stable isotope of water in different vegetation zones

Vegetation zone types	Water types	$\delta^{18}\text{O}(\text{‰})$			Coefficient of Variation	$\delta\text{D}(\text{‰})$			Coefficient of Variation
		Min	Max	Average		Min	Max	Average	
Alpine meadow	Precipitation	-31.49	14.79	-9.44	-0.70	-238.62	63.43	-59.43	-0.84
	Soil water	-12.62	-5.46	-9.16	-0.16	-83.86	-26.13	-62.92	-0.16
	Plant water	-6.68	5.12	-1.68	-2.18	-60.22	-12.14	-41.14	-0.28
	Groundwater	-10.07	-7.71	-8.84	-0.07	-68.55	43.72	-54.85	-0.10
Forest	Precipitation	-26.96	4.38	-8.63	-0.74	-205.40	41.35	-60.24	-0.87
	Soil water	-11.96	-0.07	-7.01	-0.25	-78.43	-18.48	-48.68	-0.21
	Plant water	-9.24	5.98	-5.44	-1.31	-63.29	-23.77	-45.12	-0.24
	Groundwater	-10.25	-7.43	-8.56	-0.09	-68.80	-43.75	-53.46	-0.12
Arid foothills	Precipitation	-26.47	4.24	-7.50	-0.87	-194.34	38.62	-48.62	-1.04
	Soil water	-10.98	-2.96	-8.23	-0.15	-74.22	-8.79	-59.17	-0.12
	Plant water	-9.41	2.67	-3.61	-0.88	-74.90	-29.39	-48.79	-0.23
	Groundwater	-10.34	-7.43	-8.88	-0.07	-71.67	-44.26	-55.12	-0.09

Table 3 Correlation between precipitation isotopes and different temperatures in different vegetation zones

Vegetation zone type	Correlation below	Correlation between	Correlation above	Correlation during the study period
	0°C	0°C-8°C	8°C	
	($\delta^{18}\text{O} / \delta\text{D}$)	($\delta^{18}\text{O} / \delta\text{D}$)	($\delta^{18}\text{O} / \delta\text{D}$)	
Alpine meadow	0.51*/0.59*	0.30*/0.24*	0.15/0.12	0.59*/0.61*
Forest	0.95*/0.94*	0.66*/0.69*	0.14/0.10	0.69*/0.65*
Arid foothills	0.47/0.51	0.79*/0.71*	0.31/0.14	0.83*/0.81*

Note: ** indicates a significant correlation (two-tailed) at a confidence level of 0.01, * indicates a significant correlation (two-tailed) at a confidence level of 0.05

Table 4 Correlation between different isotopes' $\delta^{18}\text{O}$ and relative humidity and precipitation in different vegetation zones

Meteorological parameters	Isotope types	Rain season			Dry season		
		Alpine meadow	Forest	Arid foothills	Alpine meadow	Forest	Arid foothills
Relative Humidity	Soil	$y = -0.001x - 8.89$, $R^2 = 0.001$	$y = -0.03x - 5.21$, $R^2 = 0.13$	$y = -0.002x - 8.01$, $R^2 = 0.002$	$y = -0.01x - 8.39$, $R^2 = 0.03$	$y = 0.01x - 7.21$, $R^2 = 0.07$	$y = -0.04x - 6.38$, $R^2 = 0.38$
		Plant	$y = -0.11x + 6.11$, $R^2 = 0.11$	$y = 0.08x - 10.53$, $R^2 = 0.13$	$y = 0.05x - 7.68$, $R^2 = 0.04$	$y = -0.09x + 3.78$, $R^2 = 0.10$	$y = -0.02x - 0.28$, $R^2 = 0.004$
	Precipitation		$y = -0.22x + 9.45$, $R^2 = 0.28$	$y = 0.02x - 9.50$, $R^2 = 0.002$	$y = 0.13x + 3.57$, $R^2 = 0.29$	$y = 0.02x - 16.47$, $R^2 = 0.002$	$y = 0.16x + 4.33$, $R^2 = 0.72$
		Soil	$y = 0.04x - 9.55$, $R^2 = 0.15$	$y = 0.02x - 7.36$, $R^2 = 0.01$	-	$y = -0.13x - 8.94$, $R^2 = 0.18$	-
	Plant		$y = -0.07x - 1.09$, $R^2 = 0.002$	$y = -0.06x - 5.01$, $R^2 = 0.01$	$y = 0.18x - 6.00$, $R^2 = 0.05$	$y = 0.07x - 2.75$, $R^2 = 0.03$	$y = -0.41x - 0.32$, $R^2 = 0.06$
		precipitation	Precipitation	$y = -0.30x - 5.21$, $R^2 = 0.09$	$y = -0.17x - 6.17$, $R^2 = 0.05$	$y = -0.28x - 2.84$, $R^2 = 0.14$	$y = -0.14x - 14.24$, $R^2 = 0.002$